Distribution of glycerol dialkyl glycerol tetraether (GDGT) lipids in a hypersaline lake system

Jingjing Li[a,b,c,d], Richard D. Pancost[b,d], B. David A. Naafs[b,d], Huan Yang[a], Cheng Zhao[c], Shucheng Xie[a*]

[a] *State Key Laboratory of Biogeology and Environmental Geology, School of Earth Sciences, China University of Geosciences, Wuhan 430074, China*

[b] *Organic Geochemistry Unit, Bristol Biogeochemistry Research Centre, University of Bristol, Bristol BS8 1TS,UK*

[c] *State Key Laboratory of Lake Sciences and Environment, Nanjing Institute of Geography and Limnology, Chinese Academy of Sciences, Nanjing 210008, China*

[d] *Cabot Institute, University of Bristol, Bristol BS8 1TH, UK*

* Corresponding author. Tel.: +86 13554116626.

E-mail address: xiecug@163.com (S.Xie).

ABSTRACT

Isoprenoid glycerol dialkyl glycerol tetraethers (isoGDGTs) of archaeal origin and branched (br)GDGTs of bacterial origin occur in a diverse range of lacustrine sedimentary environments. They have attracted attention as potential temperature proxies, providing high resolution (palaeo)environmental reconstruction from continental interiors. For this study, the distribution of GDGTs and application of GDGT-based proxies to surface samples from Chaka Salt Lake (China) as well as soils and in-flow river sediments were investigated to assess whether GDGT-based proxies are applicable to this hypersaline lake system. We show that iso- and brGDGTs are present in all sediments and soils from the Chaka Salt Lake system. GDGT-0 and crenarchaeol were generally the two most abundant isoGDGTs, suggesting *Thaumarchaeota* as a major biological source of isoGDGTs. The low ratio of crenarchaeol/crenarchaeol regioisomer suggests that *Thaumarchaeota* of the lake sediments is likely *Thaumarchaeota* group I.1b derived from the surrounding alkaline soils, arguing against the use of the TEX_{86} proxy in this system. Because alkaline soils generally have high isoGDGT concentrations, it is likely that a large allochthonous input of isoGDGTs will be a pervasive challenge to palaeoclimate applications in such settings. On the other hand, the brGDGT distributions in the lake and river sediments differed markedly from those in the surrounding soils, suggesting that instead of deriving from the surrounding soils at least part of the brGDGTs are synthesized *in situ* or delivered from more distal upland soils. Taken together, our results indicate that the mixed sources of GDGTs in Chaka Salt Lake complicate the application of GDGT-based proxies, and it will be challenging to use such proxies in this system.

Keywords: GDGT; hypersaline; lacustrine; MBT/CBT; TEX_{86}

1. Introduction

Glycerol dialkyl glycerol tetraethers (GDGTs) are core membrane-spanning lipids synthesized by Archaea and Bacteria. They are ubiquitous in the environment, occurring in marine and lacustrine sediments, and in the water column, soil, peat, hot springs, loess and stalagmites [see Schouten et al. (2013) for a review]. Isoprenoid GDGTs (isoGDGTs) are characterized by two biphytane carbon skeletons with a varying number of cyclopentane moieties, exhibit *sn*–2,3 stereochemistry (Fig. 1), and are synthesized by Archaea, including *Euryarchaeota*, *Crenarchaoeota* and *Thaumarchaeota* (Weijers et al., 2007, Pearson and Ingalls, 2013). A specific isoGDGT, crenarchaeol, containing four cyclopentane rings and one cyclohexane ring appears to be synthesized exclusively by *Thaumarchaeota* (formerly Marine Group I Crenarchaeota; Sinninghe Damsté et al., 2002, Pitcher et al., 2010). Branched GDGTs (brGDGTs) are of putative bacterial origin, exhibit *sn*–1,2 stereochemistry and feature methylated alkyl chains containing up to two cyclopentane moieties (Sinninghe Damsté et al., 2000, Weijers et al., 2006). Although the specific biological source of brGDGTs has not been identified, *Acidobacteria* are generally considered to be the likely source organisms because structural characteristics similar to those of brGDGTs were found in the lipids of subdivisions 1, 3 and 4 of this phylum (Peterse et al., 2010, Sinninghe Damsté et al., 2011, 2014).

In recent years, numerous investigations have demonstrated that GDGT-based proxies in both marine and terrestrial sedimentary environments are powerful palaeoenvironmental recorders. TEX_{86} was first established using marine sediments and is based on the distribution of cyclic moieties of isoGDGTs, biosynthesized mainly by aquatic *Thaumarchaeota* (Schouten et al., 2002, Pearson and Ingalls, 2013, Schouten et al., 2013) that are ubiquitous and abundant in marine environments (Karner et al., 2001). Although TEX_{86} was initially developed for the marine environment, the occurrence of *Thaumarchaeota* in lacustrine environments (Keough et al., 2003) led to the development of several global and regional TEX_{86} lake calibrations (Blaga et al., 2009, Powers et al., 2010, Castañeda and Schouten, 2011). Application of TEX_{86} to lakes has generated lake water temperature values consistent with other approaches, suggesting that it can be applied to certain lacustrine systems to provide a new proxy for continental palaeotemperature change (Tierney et al., 2008, 2010a, Woltering et al., 2011, Berke et al., 2012, Blaga et al., 2013). However, its application to some lakes has resulted in unreliable temperature estimates, presumably because the sediments contained isoGDGTs derived from other sources such as methanotrophs or non-aquatic *Thaumarchaeota* (Blaga et al., 2009, Pearson et al., 2011, Naeher et al., 2012, Sinninghe Damsté et al., 2012a, Naeher et al., 2014).

The methylation of branched tetraethers (MBT) and cyclization of branched tetraethers (CBT) indices were initially based on the analysis of brGDGTs in a global soil database (Weijers et al., 2007) (see Fig. 1 for GDGT structures). That work revealed that the distribution of brGDGTs in soil is strongly influenced by temperature and soil pH (Weijers et al., 2007, Peterse et al., 2012). The widespread occurrence of brGDGTs in lakes suggested that the proxy could also be applied to these systems (Blaga et al., 2009, Bechtel et al., 2010, Tierney et al., 2010b, Pearson et al., 2011, Wang et al., 2012). However, subsequent work suggested that the transfer functions originally developed for soils could systematically underestimate the actual temperature, as shown for some European and American lakes (Blaga et al., 2010), East African lakes (Tierney et al., 2010b), and Lake Lochnagar in Scotland (Tyler et al., 2010). This reflects two factors. First, brGDGT distributions differ between soil and lake sediment (Sinninghe Damsté et al., 2009, Tierney and Russell, 2009) and second, brGDGTs are evidently produced within lakes, either in the water column or in the lake sediment, making it unclear whether brGDGTs in a given setting arise from allochthonous (soil) input or *in situ* production (Tierney et al., 2010b, Loomis et al., 2011, Sinninghe Damsté et al., 2012a, Wang et al., 2012, Schoon et al., 2013). On this basis, several studies have attempted to generate regional and global lake-specific MBT(')/CBT temperature calibrations (Tierney et al., 2010b, Pearson et al., 2011, Sun et al., 2011, Loomis et al., 2012, Günther et al., 2014). Reconstructed temperatures based on these lake-specific calibrations are in good agreement with instrumental values and/or other proxy records (D'Anjou et al., 2013, Peterse et al., 2014), although some discord between estimated and actual temperatures remains (Niemann et al., 2012, Sinninghe

Damsté et al., 2012a). Hence, the mixed sources of brGDGTs in lake environments complicate their application, and more details about their distribution are required before applying them as palaoenvironmental recorders.

Although many studies have focussed on GDGTs in lacustrine settings (Blaga et al., 2009, Bechtel et al., 2010, Das et al., 2012, Wang et al., 2012, Schoon et al., 2013, Naeher et al., 2014, Peterse et al., 2014), only a few studies have examined hypersaline lake systems (Günther et al., 2014, Huguet et al., 2015). In particular, very few studies have examined brGDGTs in hypersaline lakes. We have therefore investigated the distribution and concentration of GDGTs in sediments from a hypersaline lake system (Chaka Salt Lake), as well as in inflow river sediments and soil samples collected in the catchment to the west of the lake (Fig. 2). The lake was selected because its salinity is about 10x average seawater salinity (Zheng et al., 2002). In addition, microbial data are available for the lake (Jiang et al., 2006, 2007, Yang et al., 2013), which could help to support the identification of the biological source(s) of GDGTs. Moreover, the lake is not of marine origin but evolved from an inland freshwater lake, which makes it an excellent site for studying the behaviour of GDGTs in hypersaline lacustrine environments.

2. Material and methods

2.1. Study site

Chaka Salt Lake (36°38’–36°46’N, 99°01’–99°12’E) is an athalassohaline lake (a saline lake not of marine origin) 3200 m above sea level in the southeastern edge of Qaidam Basin in northwestern China (Fig. 2). It is located between Nanshan Mountain on the northern side and Ela Mountain on the southern side. Salinity ranges between 317 and 347 psu. The area of the lake covers 105 km^2, with a catchment area of ca. 11,600 km^2. It is a hydrologically half open drainage basin with no outflow, but is fed by two freshwater rivers: Mo River and Hei River. In addition, fresh water springs feed into the lake on its northeastern and southeastern bank (Fig. 2). Local meteorological data (http://cdc.nmic.cn/home.do) indicate that the lake and surrounding area are characterized by a dry continental climate. The mean annual temperature is 5.0 °C, with the lowest mean monthly temperature of –11.2 °C in January and the highest of 19.8 °C in July. The mean temperature for summer and winter is 18.6 °C and –9.2 °C, respectively. Annual precipitation (210 mm) is greatly exceeded by evaporation (2,000 mm), causing the high salinity of the lake. The water depth is > 50 cm during the rainy season (June, July and August) and decreases to 1 cm during the dry season (January, February and March). The average lake pH is 7.0 and the pH of water from the Mo and Hei river is 7.0 and 6.8, respectively (Zheng et al., 2002, Liu et al., 2008). The soil pH of the catchment is between 7.9 and 8.4 (national soil database; http://vdb3.soil.csdb.cn/). At the time of sampling (August), the measured temperature of surface water is around 17 °C.

The landscape of the study site is dominated by alpine meadows and steppe, the vegetation type is dominated by C3 plant, mainly *Poa* sp., *Kobresia* sp., and *Oxytropis ochrocephala* (Duan et al., 2014). Typical soils are calcic brown soils and/or castanozem and all from low-density grassland covered soil.

2.2. Sampling and laboratory analysis

Four river surface sediment samples (0-2 cm), six lake surface sediment samples (0-2 cm) and five soil samples (0-2 cm) were collected in and around the lake during a field campaign in August 2011 (Fig. 2, Table 1). Samples were freeze-dried and homogenized with a mortar and pestle directly after transport to the laboratory.

Elemental and inorganic carbon (IC) were measured using a Carlo Erba EA1108 Elemental Analyzer and modified Coulomat 702 analyser, respectively. Total Organic Carbon (TOC) concentration was determined by subtracting the IC content from the total C content. TOC values represent the mean of duplicate measurements.

Samples were weighted into tin capsules and introduced into the combustion furnace (1800 °C) flushed with O_2. The combustion products were separated using gas chromatography (GC, Porpac Q column) and the composition (%) determined via thermal conductivity detection. IC was measured with a modified Coulomat 702 analyser. It was liberated as CO_2 using orthophosphoric acid and flushed with N_2 into the coulomatic cell set to known pH (9.2), resulting in a decrease in pH. The magnitude of the current applied to return the cell to its original value is directly proportional to the IC released as CO_2.

Lipid extraction generally followed Yang et al. (2012) with some modifications. Each sample (ca. 10 g) was ultrasonically extracted 6x with dichloromethane DCM/MeOH (9:1, v/v). The total lipid extract (TLE) was concentrated using rotary evaporation under vacuum and separated using column chromatography with silica gel as stationary phase and hexane/DCM (9:1, v/v) and DCM/MeOH (9:1, v/v) to yield an apolar and a polar fraction, respectively. The polar fraction, containing the GDGTs, was filtered over a 0.45um PTFE filter with hexane/isopropanol (99:1, v/v) and dried under N_2 prior to analysis using high performance liquid chromatography/atmospheric pressure chemical ionisation mass spectrometry (HPLC-APCI-MS).

GDGT analysis was performed with an Agilent 1200 series liquid chromatograph connected to a triple quadrupole mass spectrometer, using single ion monitoring (SIM) mode and *m/z* 1302, 1300, 1298, 1296, 1294, 1292, 1050, 1048, 1046, 1036, 1034, 1032, 1022, 1020, 1018 and 744, 653 to enhance sensitivity. Separation was achieved using an Alltech Prevail Cyano column (150 × 2.1 mm, 3 μm), following the method of Yang et al. (2014). Quantification was obtained by addition of an internal synthetic C_{46} GDGT standard (cf. Huguet et al., 2006). The final quantification was semi-quantitative as we did not determine the relative response factor between GDGTs and the standard. For determination of ACE (see below), the response factors for archaeol and GDGT-0 were assumed to be identical

2.3. Calculation of GDGT indices and proxies

Indices based on the distribution of GDGTs were calculated according to previous studies, TEX_{86} was calculated following the equation of Schouten et al. (2002), the Roman and Arabic numerals correspond to GDGT structures in Fig. 1:

$$TEX_{86} = \frac{\text{GDGT}-2 + \text{GDGT}-3 + \text{Cren}'}{\text{GDGT}-1 + \text{GDGT}-2 + \text{GDGT}-3 + \text{Cren}'} \quad (1)$$

The soil input index, BIT was calculated following the equation of Hopmans et al. (2004):

$$\text{BIT} = \frac{\text{GDGT}-\text{I} + \text{GDGT}-\text{II} + \text{GDGT}-\text{III}}{\text{GDGT}-\text{I} + \text{GDGT}-\text{II} + \text{GDGT}-\text{III} + \text{Cren}} \quad (2)$$

The MBT and CBT indices were calculated as follows (Weijers et al., 2007):

$$\text{MBT} = \frac{([\text{I}] + [\text{Ib}] + [\text{Ic}])}{([\text{I}] + [\text{Ib}] + [\text{Ic}] + [\text{II}] + [\text{IIb}] + [\text{IIc}] + [\text{III}] + [\text{IIIb}] + [\text{IIIc}])} \quad (3)$$

$$\text{CBT} = -\log\left(\frac{([\text{Ib}]+[\text{IIb}])}{([\text{I}]+[\text{II}])}\right) \quad (4)$$

The revised MBT’ was calculated according to the equation developed by Peterse et al. (2012):

$$\text{MBT}' = \frac{([\text{I}] + [\text{Ib}] + [\text{Ic}])}{([\text{I}] + [\text{Ib}] + [\text{Ic}] + [\text{II}] + [\text{IIb}] + [\text{IIc}] + [\text{III}])} \quad (5)$$

The ratio of total isoGDGTs and total brGDGTs index, $R_{i/b}$ was calculated according to the equation of Xie et al. (2012):

$$R_{i/b} = \frac{\sum \text{isoGDGTs}}{\sum \text{brGDGTs}} \quad (6)$$

The ratio of archaeol and GDGT-0 index, ACE was calculated according to the equation of Turich and Freeman (2011), except that the multiplication by 100 has been removed to make it more consistent with other GDGT-based indices.

$$\mathrm{ACE} = \frac{\mathrm{archaeol}}{\mathrm{archaeol+GDGT-0}} \tag{7}$$

We note that recent analytical developments have revealed that the pentamethylated and hexamethylated brGDGTs actually comprise multiple structural isomers, with methylation at either C-5 or C-6 (De Jonge et al., 2013).This has resulted in a new soil calibration (De Jonge et al., 2014a) but not new lake calibrations. Here, we applied the original analytical approaches and calibrations, in which C-5 and C-6 isomers are integrated together.

TEX_{86} inferred lake surface temperature (LST) was calculated using Eqs. 8-12 (Powers et al., 2010, Tierney et al., 2010a, Castañeda and Schouten, 2011). Specific calibrations for summer (SLST) and winter lake surface temperature (WLST) were used to infer seasonal temperatures (Powers et al., 2010).

$$\mathrm{LST_{Powers2010}} = 50.8 \times \mathrm{TEX_{86}} - 10.4 \tag{8}$$

$$\mathrm{SLST_{Powers2010}} = 46.6 \times \mathrm{TEX_{86}} - 5.6 \tag{9}$$

$$\mathrm{WLST_{Powers2010}} = 57.3 \times \mathrm{TEX_{86}} - 17.5 \tag{10}$$

$$\mathrm{LST_{Tierney2010}} = 38.87 \times \mathrm{TEX_{86}} - 3.50 \tag{11}$$

$$\mathrm{LST_{Castañeda2011}} = 54.89 \times \mathrm{TEX_{86}} - 13.36 \tag{12}$$

MBT'/CBT inferred mean annual air temperature (MAAT) was calculated for the soil and lake sediments. Based on a globally distributed soil calibration (Weijers et al., 2007), MAAT can be obtained using Eq. 13. This calibration was extended and revised with a new transfer function (Eq. 14) by Peterse et al. (2012). In addition, new (local) calibrations were proposed by Yang et al. (2014) for semiarid and arid regions of China (Eq. 15 and 16).

$$\mathrm{MAAT_{Weijers2007}} = (\mathrm{MBT} - 0.12 - 0.19 \times \mathrm{CBT})/0.02 \tag{13}$$

$$\mathrm{MAAT_{Peterse2012}} = 0.81 - 5.67 \times \mathrm{CBT} + 31.0 \times \mathrm{MBT'} \tag{14}$$

$$\mathrm{MAAT_{Yang2014}} = 7.5 + 16.1 \times \mathrm{MBT} - 1.2 \times \mathrm{CBT} \tag{15}$$

$$\mathrm{MAAT_{Yang2014'}} = 20.9 - 13.4 \times f(\mathrm{II}) - 17.2 \times f(\mathrm{III}) - 17.5 \times f(\mathrm{IIb}) + 11.2 \times f(\mathrm{Ib}) \tag{16}$$

All samples were analysed in duplicate and the data are presented as the mean of these duplicates. The average analytical duplicate error for GDGT-based indices was < 0.01.

Several global and regional lake temperature calibration studies have been proposed for African lakes (Tierney et al., 2010b, Loomis et al., 2012), Chinese and Nepalese lakes (Sun et al., 2011) and lakes along a transect from the Scandinavian Arctic to Antarctica (Pearson et al., 2011), in addition the newly developed calibration for Tibetan Plateau (Günther et al., 2014):

$$\mathrm{MAAT_{Tierney2010}} = 11.8 + 32.5 \times \mathrm{MBT} - 9.3 \times \mathrm{CBT} \tag{17}$$

$$\mathrm{MAAT_{Tierney2010'}} = 50.5 - 74.2 \times f(\mathrm{III}) - 31.6 \times f(\mathrm{II}) - 34.7 \times f(\mathrm{I}) \tag{18}$$

$$\mathrm{MAAT_{Sun2011}} = 4.0 + 38.2 \times \mathrm{MBT} - 5.6 \times \mathrm{CBT} \tag{19}$$

$$\mathrm{MAAT_{Pearson2011}} = 20.9 + 98.1 \times f(\mathrm{Ib}) - 12.0 \times f(\mathrm{II}) - 20.5 \times f(\mathrm{III}) \quad (20)$$

$$\mathrm{MAAT_{Loomis2012}} = 2.5 + 45.3 \times \mathrm{MBT} - 5.0 \times \mathrm{CBT} \quad (21)$$

$$\mathrm{MAAT_{Loomis2012'}} = 36.9 - 50.1 \times f(\mathrm{III}) - 35.5 \times f(\mathrm{II}) - 1.0 \times f(\mathrm{I}) \quad (22)$$

$$\mathrm{MAAT_{Günther2014}} = -3.84 + 9.84 \times \mathrm{CBT} + 5.92 \times \mathrm{MBT'} \quad (23)$$

where f is the fractional abundance of a specific brGDGT relative to total brGDGTs. Note that in the above equations (and below), we use the prime symbol (i.e. $\mathrm{MAAT_{Tierney2010}}$ and $\mathrm{MAAT_{Tierney2010'}}$) to indicate calibrations that directly use fractional abundance of brGDGTs as opposed to MBT values.

3. Results

3.1. Concentration and distribution pattern of isoGDGTs

All samples contained isoGDGTs, but the concentration, normalized to total organic carbon (TOC), varied substantially (Table 1 and Fig. 3). The summed concentration (semi-quantitatively determined) in soils ranged from 80 to 1050 ng/g TOC, lower than concentrations in river and lake sediments, which varied from 580 to 2040 ng/g TOC and 60 to 2560 ng/g TOC, respectively. GDGT-0 was generally the most abundant isoGDGT both in river (50–80% of major isoGDGTs) and lake sediments (30–75%), with one exception in sample LS10 where crenarchaeol (33%) was the dominant isoGDGT (Table 1). The concentration of isoGDGTs with cyclopentane(s) moieties (isoGDGT 1-3) was low in most river and lake sediment samples. In river sediments, the relative abundance of crenarchaeol is higher than GDGT-1, GDGT-2 and GDGT-3. In contrast, lake sediments contained more complex distributions (Table 1); for example, crenarchaeol was generally more abundant than isoGDGTs 1-3, but the proportion of GDGT-1 was higher than that of crenarchaeol in samples LS5, LS8 and LS9 (Table 1, Fig. 3). The distribution pattern of isoGDGTs in soils was also variable. Crenarchaeol dominated in samples S11, S12, S14, whereas GDGT-0 was the most abundant in S13 and S15 (Table 1, Fig. 3).

TEX_{86} values for river sediments and soils were almost identical at 0.68 ± 0.03 and 0.69 ± 0.05, respectively (Table 1). The TEX_{86} values for lake sediments show high variability, ranging from 0.28 to 0.72. The ACE index, based on the relative abundance of archaeol and GDGT-0, was determined for river sediments, lake sediments and soils. ACE indices for river sediments and soils are generally lower than those of lake sediments, ranging from 0.01 to 0.18 in river sediment and from 0.01 to 0.14 in soils (Table 1). Indeed, the amount of archaeol in soil sample S14 is quite low, and the ACE index of S14 is close to 0. In contrast, the ACE values of lake sediments are generally higher than river sediments and soils (Table 1), varying from 0.16 to 0.66.

3.2. Concentration and distribution pattern of brGDGTs

The concentration of total brGDGTs in river sediments, lake sediments and soils varied from 640-3300 ng/g TOC, 30-1740 ng/g TOC and 20-910 ng/g TOC respectively

(Table 2, Fig. 3). In contrast to the lower concentration of isoGDGTs in soils than sediments, the total concentration of brGDGTs in river samples was higher than in lake sediments and soils. The brGDGTs without cyclopentane moieties (GDGT I, II, and III) were generally more abundant than cyclopentane ring-containing brGDGTs.

MBT indices for river and lake sediments were similar at 0.20 ± 0.02 and 0.16 ± 0.06, respectively. MBT for soils was lower, with values of 0.07 ± 0.01. Due to the low concentration of GDGT-IIIb and –IIIc for all samples, MBT' was almost identical to MBT (Table 2). CBT values were also similar for river and lake sediments at 0.22 ± 0.09 and 0.32 ± 0.23, respectively. CBT for soils was much higher at 1.26 ± 0.20 (Table 2). BIT values for river sediments, lake sediments and soils were 0.77 ± 0.11, 0.68 ± 0.18, and 0.57 ± 0.09, respectively (Table 1) – intriguingly, BIT values are lowest in the soils. The $R_{i/b}$ index for river sediments, lake sediments and soils was 0.95 ± 0.27, 5.75 ± 5.34 and 2.48 ± 1.45, respectively.

4. Discussion

4.1. Potential biological sources of isoGDGTs

4.1.1. GDGT-0

GDGT-0 has a wide range of biological sources. It is produced by all major groups of archaea except for halophilic archaea, although it has been found in halophilic environments (Turich and Freeman, 2011, Schouten et al., 2013). Despite that, the likely biological sources of GDGT-0 in terrestrial settings appear to be mainly methanogens and *Thaumarchaeota* (Blaga et al., 2009). The ratio of GDGT-0/crenarchaeol has been proposed to evaluate the contribution of GDGT-0 produced by methanogens and a value > 2 is generally thought to reflect a substantial contribution from methanogens to the isoGDGT pool (Blaga et al., 2009, Bechtel et al., 2010). The ratio was generally < 2 for our soil samples (except for one sample S15, Table 1), similar to the value for the catchment soils from other lakes (Naeher et al., 2014), suggesting that GDGT-0 in the surface of soils of our hypersaline lake system is derived mainly from *Thaumarchaeota*. However the ratio was > 6 for S15, indicating that this soil could contain a significant amount of methanogens. The soils span a range of different types of calcic brown soils and/or castanozem, and all come from low-density grassland covered soil, indicating there must be additional factors other than soil type and vegetation type that determine the isoGDGT composition in soils.

The GDGT-0/crenarchaeol ratios in river sediments were much higher than those of the soils, with values between 1.7 and 7.1 (Table 1), suggesting that methanogens were a main source of GDGT-0. In comparison, the ratio in lake sediments was highly variable. For LS6, LS7 and LS10, it varied between 0.9 and 2.2. These values are similar to those for the surrounding soils and river sediments, indicating these lake sediments could contain significant contribution of *Thaumarchaeota*. However, some lake sediments were characterized by much higher ratio values, between 16.3 and 52.4

for LS5, LS8, and LS9. These are similar to those reported from European lake sediments (Blaga et al., 2009) and indicate that methanogens are likely a major source of GDGT-0 in at least some of our lake sediments. These results suggest that there must be some methanogens with high salinity tolerance and which produce GDGT-0 in this hypersaline setting. However, the contribution of other types of halophilic archaea cannot be excluded. Although GDGT-0 has not been detected in cultures of these organisms, uncultured halophiles could be the producers of GDGT-0 in hypersaline settings (Turich and Freeman, 2011, Birgel et al., 2014, Huguet et al., 2015). Indeed, there is an increasing number of studies showing the potential of halophilic archaea to produce biphytanes (see Turich and Freeman (2011) and references therein).

Microbial diversity analyses of water and sediments from the lake demonstrate that the majority of archaeal clone sequences in the sediments are related to methanogens and only a small proportion of sequences was affiliated with the *Crenarchaeota* group (Jiang et al., 2006), probably indicating the contribution of GDGT-0 from *Crenarchaeota* is less than methanogens. The phylogenetic compositions of the archaeal clone libraries of lake water show a distinct difference, all archaeal clone sequences for lake water were related to the *Halobacteriales* group due to high salinity (Jiang et al., 2006). However, only a small percentage of sequences was related to *Halobacteriales* for lake sediments (Jiang et al., 2006), indicating the production of GDGT-0 from uncultured halophiles could not be excluded. Taken together our results indicate that

GDGT-0 in river and lake sediments is derived predominantly from methanogens with high salinity tolerance and allochthonous *Thaumarchaeota* sources.

4.1.2. Crenarchaeol and crenarchaeol regioisomer

Crenarchaeol and its regioisomer are considered to be synthesized uniquely by the phylum *Thaumarchaeota* (NH_4^+ oxidizing archaea) in aquatic and terrestrial environments including the water column, sediments and soils, and they have been found in all cultures of *Thaumarchaeota* (see Schouten et al., 2013 and references therein). Recent research suggests that it could also be synthesized by Marine Group II *Euryarchaeota* (Lincoln et al., 2014a), but that study is controversial (Lincoln et al., 2014b, Schouten et al., 2014). Several studies have shown that significant quantities of the regioisomer (relative to crenarchaeol) are produced by soil *Thaumarchaeota* group I.1b, in contrast to the low amount normally found in (aquatic) *Thaumarchaeota* group I.1a (Kim et al., 2012, Sinninghe Damsté et al., 2012b). Therefore, we use the ratio of crenarchaeol and its regioisomer (cren/cren') to distinguish the type of *Thaumarchaeota* (Sinninghe Damsté et al., 2012a, Liu et al., 2013). Based on published data, we propose that values >25 are indicative for *Thaumarchaeota* group I.1a and markedly lower ones indicative for group I.1b (Fig. 4, Table A1 in Supplementary material). An overview of reported values shows that cren/cren' in soils is generally much lower than for lake and marine sediments (Fig. 4). The values for our river sediments, lake sediments and soils are similar: 13.3 ± 2.0, 10.2 ± 2.8 and 21.8 ± 6.9, respectively. Interestingly the values in the soils are higher than for the river and lake sediments (Table 1), but are all < 25. This suggests that *Thaumarchaeota* in the Chaka Salt Lake system are dominated by group I.1b *Thaumarchaeota*.

As halophiles are not known to produce crenarchaeol or its regioisomer, and the cren/cren' ratios in our lake sediments are similar to those in river sediments and soils, we suggest that in the lake sediments crenarchaeol and its regioisomer derive predominantly from either surrounding soils or riverine input. This is supported by genomic data that indicate that the functional gene encoding for the first step in NH_4^+ oxidation for *Thaumarchaeota* (*amoA*) was not present in water and sediment samples from Chaka Salt Lake (Yang et al., 2013).

4.1.3. IsoGDGT-1 to 3

Significant amounts of isoGDGTs 1-3, containing cyclopentane moieties, were present in all samples. They can derive from both *Thaumarchaeota* and methanogens (and also anaerobic methanotrophs; Pancost et al., 2001, Schouten et al., 2013) and further investigation is required to verify their biological sources. As shown in Fig. 3, the average proportion of GDGT-1, GDGT-2 and GDGT-3 for each setting was similar, although the proportion of GDGT-1 in lake sediments was higher than the other two settings, leading to a relatively low TEX_{86} for lake sediments. Regardless of source, the average proportion of these isoGDGTs is roughly similar in river sediments and soils, suggesting that these isoGDGTs, like crenarchaeol, likely derive from the surrounding soils.

4.1.4. Overview of isoGDGT sources

It seems likely that the predominance of isoGDGTs in lake sediments, especially crenarchaeol and isoGDGTs 1-3, are derived from soils. It is likely that this arises from their atypically high concentration in the surrounding soils (Table 1). In fact, the average concentration of crenarchaeol in the soils (260 ng/g TOC) was higher than that in river (230 ng/g TOC) and lake sediments (110 ng/g TOC). This strong crenarchaeol contribution to the soils is evident from their relatively low BIT indices (0.57 ± 0.09) compared to previously investigated soils in which BIT indices are normally >0.9 (see Schouten et al. (2013) and references therein). Although this particular effect could be site-specific, we suggest that it could be characteristic of many hypersaline lake systems, because a relatively high concentration of crenarchaeol and relatively low concentration of brGDGTs is characteristic of arid environments and alkaline soils (Yang et al., 2014).

4.2. Potential biological sources of brGDGTs

The distribution of brGDGTs, illustrated for example by a cross plot of MBT and CBT indices (Fig. 5), was markedly different between soils and sediments. The different distribution suggests that there is a contribution of *in situ* produced brGDGTs to the river and lake sediments and that the brGDGTs do not originate solely from the surrounding soils. The average brGDGT concentration for lake sediments is also higher than that for soils (Table 1), further indicating that a significant amount of brGDGTs is produced within Chaka Salt Lake. These results are consistent with those from other river and lake systems where brGDGTs are produced *in situ* (Zell et al., 2013, De Jonge et al., 2014b).

GDGT distributions are also consistent with separate lake and soil sources. The distribution of brGDGTs in the sediments is similar to that in lakes from around the world, with GDGT-II dominating (Tierney et al., 2010b, Tyler et al., 2010, Loomis et al., 2011, Pearson et al., 2011, Sun et al., 2011, Schoon et al., 2013, Loomis et al., 2014). In contrast, the most abundant brGDGT in surrounding soils is GDGT-III. This further supports our suggestion that brGDGTs in our lake sediment samples were derived from *in situ* production, either in the lake water column or sediments. However, as discussed above, brGDGT distributions do differ. Although brGDGTs II and III are the most abundant in sediments and soils, in sediments GDGT II is nearly as abundant as GDGT III whereas it is less abundant than GDGT III in soils (Fig. 3). The dominance of GDGT III, followed by GDGT-II and GDGT-I, in soils is similar to that reported for soils from dry and cold regions like high altitude regions in Norway (Peterse et al., 2009), western states from the USA (Dirghangi et al., 2013) and Qinghai-Tibetan Plateau, China (Liu et al., 2013).

A complication is that microbial ecological analysis of this lake suggested that the majority of bacteria in the water and sediments were *Bacteroidetes* and low G + C gram positive bacteria, respectively (Jiang et al., 2006), and not *Acidobacteria*, a presumed biological source of brGDGTs (Sinninghe Damsté et al., 2011, 2014). This would suggest that either the brGDGTs in sediments from Chaka Salt Lake are derived from riverine sources and/or are produced *in situ* by organisms other than *Acidobacteria*. Moreover, it is not known if the microbial communities differ between the dry and rainy season; although both biomarker and microbial ecology sampling was conducted during the rainy season, it is possible that brGDGTs were generated at another time under different conditions. Further testing is required to differentiate these possibilities.

4.3. Implications for application of GDGT proxies

4.3.1. BIT

The BIT index was originally developed to trace the input of soil organic matter (OM) to aquatic environments. Values close to 1 (absence of crenarchaeol) are typical for soils, whereas values close to 0 are typical for open marine and large lake sediments (Hopmans et al., 2004). For Chaka Salt Lake the BIT values of river (0.77 ± 0.11) and lake sediments (0.68 ± 0.18) were higher than those of soil (0.57 ± 0.09). Previous studies have shown that the BIT index in soils is influenced by pH, with values decreasing in Chinese soils with pH > 5.5 (Yang et al., 2012); given the high pH values for soils surrounding Chaka Salt Lake, that is likely the explanation here. The predominance of isoGDGTs over brGDGTs in alkaline soils, in contrast to the brGDGT dominance in acid and neutral soils (Yang et al., 2014), is also reflected in higher $R_{i/b}$ ratios (Xie et al., 2012).

It seems that alkaline soils favor the growth of archaeal community, and especially *Thaumarchaeota* (Bates et al., 2011). Hence, the alkaline conditions in soils from the catchment area of Chaka Salt Lake (with pH around 8), will likely favor the growth of *Thaumarchaeota*, leading to the high amounts of crenarchaeol (and other isoGDGTs) we observe in our samples. Consequently, the limitations of the BIT index are likely relevant for other arid systems – and other hypersaline lakes.

4.3.2. TEX_{86}

The applicability of TEX_{86} is constrained by a variety of factors (see Schouten et al. (2013) and references therein), but the sources of isoGDGTs are considered to be particularly important in continental archives. It is not suitable to apply calibrations of TEX_{86} in lacustrine environments if the lake sediments contained large amounts of likely soil-derived isoGDGTs (Blaga et al., 2009, Powers et al., 2010), or if the lakes have been strongly influenced by methanogenesis (Blaga et al., 2009). Here we tested the applicability of TEX_{86} to reconstruct lake water temperature in Chaka Salt Lake.

Interestingly, given the high allochthonous and methanogen inputs (see above), the reconstructed temperatures based on several lake calibrations (Powers et al., 2010, Tierney et al., 2010a, Castañeda and Schouten, 2011) are consistent with the measured surface water temperature of 17 °C (Fig. 6, and Table A2 in Supplementary material). The reconstructed summer lake surface temperature (Powers et al., 2010) is around 18 ± 10 °C, similar to the measured surface water temperature (Fig.6). Given the strong evidence that isoGDGTs derive from surrounding soils rather than the lake, we interpret the agreement between TEX_{86}-derived temperatures and lake temperatures as coincidental. Instead, this likely reflects the fact that TEX_{86} values in soil can record soil temperatures (Yang et al., 2016). Indeed, using the relationship obtained for an altitudinal transect of Mt Xiangpi in China (Liu et al., 2013, Yang et al., 2016), our TEX_{86} values yield MAT of -2 ± 3 °C, close to the observed MAAT of 5 °C.

4.3.3. ACE

The relative abundance of archaeol to GDGT-0, the ACE index (Equation 7), was originally proposed to track increasing salinity in marine and hypersaline environments (Turich and Freeman, 2011). ACE also appears to successfully document salinity change in northeastern Tibetan lakes and soils (Wang et al., 2013). However, Günther et al. (2014) showed that in southwestern Tibetan saline high mountain lakes, the relationship between the ACE index and salinity was complex (Günther et al., 2014).

Similarly, in tropical ponds, high ACE indices (between ca. 0.9 and 1) occur in ponds with markedly contrasting salinity, including low salinity, suggesting that it is not applicable to such settings (Huguet et al., 2015).

In our study, ACE indices of lake sediments (mean values 0.41) are higher than river sediments (mean value 0.09) and soils (mean value 0.03) (Table 1), as expected (although one river sediment RS4 has a higher ACE index of 0.18). However, the ACE indices of Chaka Salt Lake system are generally lower than those from marine environments (Turich and Freeman, 2011, Huguet et al., 2015), even though the water salinity of Chaka Salt Lake is ~10x higher. A high contribution of isoGDGTs, especially GDGT-0 from surrounding alkaline soils, as appears to be the case here, could bias the application of ACE index in lake sediments towards low values. This indicates that the sources of GDGT-0 in various saline environments should be constrained before the ACE index can be applied as a salinity proxy.

4.3.4. MBT'/CBT

In general, lake sediments from cold regions are dominated by brGDGT-III, whereas those from warmer regions are dominated by brGDGT-I (Tierney et al., 2010b, Loomis et al., 2011, Sun et al., 2011, Shanahan et al., 2013), in-line with the overall temperature dependence of brGDGTs with an increase in the degree of methylation at lower temperatures. Here, the relative abundance of GDGT-I was lower than GDGT-III in both river and lake sediments (Fig. 3), in agreement with the low-temperature continental climate of the region and mean annual water temperature of the lake of 5.0°C.

Temperatures derived from brGDGT distributions in soils range between -17.0 and -11.3 °C (Table A2 in Supplementary material), when applying the original global soil calibration (Weijers et al., 2007) and -5.7 to -2.3 °C with the revised calibration (Peterse et al., 2012) (Fig. 7). Both are markedly lower than the instrumental MAAT of 5 °C and lower than any modern soils in the calibration data set. In contrast to the global soil calibrations, application of the regional soil calibration (Yang et al., 2014) yields reconstructed temperatures more similar to the instrumental MAAT (Fig. 7). We conclude that this better agreement is especially due to the fact that these regional soil calibrations account for the impact of aridity on brGDGT distributions, which is known to lead to an underestimation of MAAT (Peterse et al., 2012).

As discussed above (Sections 4.2 and 4.3.1), brGDGTs in river and lake sediments appear not to derive from surrounding soils, but we cannot rule out the possibility of an upland soil source. Therefore, we calculated MAAT of the sediments by using soil-based calibrations (Fig. 7). Application of the original MBT-CBT calibration of Weijers et al. (2007) to river and lake sediments yielded temperatures of 1.8 and -1.2 °C respectively, slightly cooler than observed MAAT, taking into account the calibration error (ca. 5 °C) (Fig. 7). Applying the revised MBT’-CBT calibration of Peterse et al.

(2012) to river and lake sediments yielded warmer reconstructed MAATs (5.9 and 4.1 °C) that were similar to observed MAAT.

In contrast, the regional soil calibration of Yang et al. (2014) resulted in relatively high MAATs (9.0 -10.4 °C), higher in fact by 3.8-5.4 °C than observed MAAT (Fig. 7). Therefore, among soil calibrations, it is the global calibration of Peterse et al. (2012) that is most consistent with MAATs in the Chaka Salt Lake catchment, even though soils of this area are not included in the global calibration. We suggest that this is because the regional Chinese calibration of Yang et al. (2014) is dominated by arid soils that are not representative of inputs to Chaka Salt Lake. Although the lake is surrounded by arid and alkaline soils, the brGDGTs in its sediments do not appear to derive from them, as discussed above. Instead, brGDGTs could derive from upland soils from less arid settings, such that a global calibration is more appropriate.

Alternatively, the brGDGTs could be produced *in situ* in lake sediments. To explore this, we applied various MAAT lake calibrations to the river and lake sediments (Fig. 8), but these all yielded temperature values (significantly) higher than observed MAAT. The best fit to a MAAT of 5 °C was obtained using the calibration of (Sun et al., 2011), which generated MAATs of 10.3 ± 1.1 °C and 8.2 ± 3.3 °C for river sediments and lake sediments, respectively. Therefore, unless a strong summer production bias is invoked, lake-based calibrations do not appear applicable to Chaka Salt Lake.

Therefore, the global soil calibrations appear to be most relevant Chaka Salt Lake –

although that also assumes an input from upland rather than local soils. Although that is speculative, it is consistent with the lack of putative brGDGT-producing bacteria in the lake. If so, it suggests that the MBT/CBT palaeothermometer can be used in hypersaline systems, avoiding aridity biases that impact local soils, but it must be done so cautiously given the complex controls on how such signals are carried through catchments.

5. Conclusions

We investigated the distributions of isoprenoid and branched GDGTs in river sediments, lake sediments and soils from Chaka Salt Lake, an inland hypersaline lake in China. Our work indicates that the GDGTs present in hypersaline lakes reflect both the high salinity conditions of the lake but also the processes that govern GDGT distributions and transport in the surrounding arid environment. We demonstrated that methanogens likely had a significant contribution to the isoGDGT pool of the river and lake sediments. Based on the low cren/cren' ratio in all samples, *Thaumarchaeota* group I.1b likely were another major isoGDGT source, primarily from the surrounding alkaline soils. This also appears to have biased the ACE Index, with high allochthonous GDGT-0 inputs yielding lower-than-expected values. The brGDGT distributions in lake and river sediments differed markedly from surrounding soils, and higher concentration of brGDGTs occurred in lake sediments than soils, suggesting that at least part of the brGDGTs were synthesized in either the lake or river. However, the contribution of brGDGTs from upland soils cannot be excluded, and MAATs derived from lake sediment brGDGTs appear to be consistent with such an origin.

Acknowledgements

We would like to thank F. Zheng, J. Xue, X. Qiu, H. Zhang, J. Lu and M. Huang for sample collection and W. Ding for help with LC-MS maintenance. The work was supported by the State Key R&D Program (grant No. 2016YFA0601104), Natural Science Foundation of China (grants No. 41330103 and 41502173) and 111 Project (grant No. B08030). We thank two anonymous reviewers for constructive and valuable comments, which significantly improved the manuscript.

References

Bates, S.T., Berg-Lyons, D., Caporaso, J.G., Walters, W.A., Knight, R., Fierer, N., 2011. Examining the global distribution of dominant archaeal populations in soil. The ISME journal 5, 908-917.

Bechtel, A., Smittenberg, R.H., Bernasconi, S.M., Schubert, C.J., 2010. Distribution of branched and isoprenoid tetraether lipids in an oligotrophic and a eutrophic Swiss lake: insights into sources and GDGT-based proxies. Organic Geochemistry 41, 822-832.

Berke, M.A., Johnson, T.C., Werne, J.P., Grice, K., Schouten, S., Sinninghe Damsté, J.S., 2012. Molecular records of climate variability and vegetation response since the Late Pleistocene in the Lake Victoria basin, East Africa. Quaternary Science Reviews 55, 59-74.

Birgel, D., Guido, A., Liu, X., Hinrichs, K.-U., Gier, S., Peckmann, J., 2014. Hypersaline conditions during deposition of the Calcare di Base revealed from archaeal di- and tetraether inventories. Organic Geochemistry 77, 11-21.

Blaga, C.I., Reichart, G.-J., Heiri, O., Damsté, J.S.S., 2009. Tetraether membrane lipid distributions in water-column particulate matter and sediments: a study of 47 European lakes along a north–south transect. Journal of Paleolimnology 41, 523-540.

Blaga, C.I., Reichart, G.-J., Schouten, S., Lotter, A.F., Werne, J.P., Kosten, S., Mazzeo, N., Lacerot, G., Damsté, J.S.S., 2010. Branched glycerol dialkyl glycerol tetraethers in lake sediments: Can they be used as temperature and pH proxies? Organic Geochemistry 41, 1225-1234.

Blaga, C.I., Reichart, G.-J., Lotter, A.F., Anselmetti, F.S., Sinninghe Damsté, J.S., 2013. A TEX86 lake record suggests simultaneous shifts in temperature in Central Europe and Greenland during the last deglaciation. Geophysical Research Letters 40, 948-953.

Castañeda, I.S., Schouten, S., 2011. A review of molecular organic proxies for examining modern and ancient lacustrine environments. Quaternary Science Reviews 30, 2851-2891.

D'Anjou, R., Wei, J., Castaneda, I., Brigham-Grette, J., Petsch, S., Finkelstein, D., 2013. High-latitude environmental change during MIS 9 and 11: biogeochemical evidence from Lake El'gygytgyn, Far East Russia. Climate of the Past 9, 567-581.

Das, S.K., Bendle, J., Routh, J., 2012. Evaluating branched tetraether lipid-based palaeotemperature proxies in an urban, hyper-eutrophic polluted lake in South Africa. Organic Geochemistry 53, 45-51.

De Jonge, C., Hopmans, E.C., Stadnitskaia, A., Rijpstra, W.I.C., Hofland, R., Tegelaar, E., Damsté, J.S.S., 2013. Identification of novel penta-and hexamethylated branched glycerol dialkyl glycerol tetraethers in peat using HPLC–MS 2, GC–MS and GC–SMB-MS. Organic Geochemistry 54, 78-82.

De Jonge, C., Hopmans, E.C., Zell, C.I., Kim, J.-H., Schouten, S., Damsté, J.S.S., 2014a. Occurrence and abundance of 6-methyl branched glycerol dialkyl glycerol tetraethers in soils: Implications for palaeoclimate reconstruction. Geochimica et Cosmochimica Acta 141, 97-112.

De Jonge, C., Stadnitskaia, A., Hopmans, E.C., Cherkashov, G., Fedotov, A., Damsté, J.S.S., 2014b. In situ produced branched glycerol dialkyl glycerol tetraethers in suspended particulate matter from the Yenisei River, Eastern Siberia. Geochimica et Cosmochimica Acta 125, 476-491.

De La Torre, J.R., Walker, C.B., Ingalls, A.E., Könneke, M., Stahl, D.A., 2008. Cultivation of a thermophilic ammonia oxidizing archaeon synthesizing crenarchaeol. Environmental Microbiology 10, 810-818.

Dirghangi, S.S., Pagani, M., Hren, M.T., Tipple, B.J., 2013. Distribution of glycerol dialkyl glycerol tetraethers in soils from two environmental transects in the USA. Organic Geochemistry 59, 49-60.

Duan, Y., Zhao, Y., Sun, T., Zhang, X., 2014. δD values of individual n-alkanes in sediments from the Chaka salt lake (China) and terrestrial plants from the surrounding area. Geochemical Journal 48, 321-329.

Günther, F., Thiele, A., Gleixner, G., Xu, B., Yao, T., Schouten, S., 2014. Distribution of bacterial and archaeal ether lipids in soils and surface sediments of Tibetan lakes:

implications for GDGT-based proxies in saline high mountain lakes. Organic Geochemistry 67, 19-30.

Hopmans, E.C., Weijers, J.W.H., Schefuß, E., Herfort, L., Sinninghe Damsté, J.S., Schouten, S., 2004. A novel proxy for terrestrial organic matter in sediments based on branched and isoprenoid tetraether lipids. Earth and Planetary Science Letters 224, 107-116.

Huguet, A., Grossi, V., Belmahdi, I., Fosse, C., Derenne, S., 2015. Archaeal and bacterial tetraether lipids in tropical ponds with contrasting salinity (Guadeloupe, French West Indies): Implications for tetraether-based environmental proxies. Organic Geochemistry 83–84, 158-169.

Huguet, C., Hopmans, E.C., Febo-Ayala, W., Thompson, D.H., Sinninghe Damsté, J.S., Schouten, S., 2006. An improved method to determine the absolute abundance of glycerol dibiphytanyl glycerol tetraether lipids. Organic Geochemistry 37, 1036-1041.

Jiang, H., Dong, H., Zhang, G., Yu, B., Chapman, L.R., Fields, M.W., 2006. Microbial diversity in water and sediment of Lake Chaka, an athalassohaline lake in northwestern China. Applied and environmental microbiology 72, 3832-3845.

Jiang, H., Dong, H., Yu, B., Liu, X., Li, Y., Ji, S., Zhang, C.L., 2007. Microbial response to salinity change in Lake Chaka, a hypersaline lake on Tibetan plateau. Environmental Microbiology 9, 2603-2621.

Jung, M.-Y., Park, S.-J., Min, D., Kim, J.-S., Rijpstra, W.I.C., Sinninghe Damsté, J.S., Kim, G.-J., Madsen, E.L., Rhee, S.-K., 2011. Enrichment and Characterization of an Autotrophic Ammonia-Oxidizing Archaeon of Mesophilic Crenarchaeal Group I.1a from an Agricultural Soil. Applied and Environmental Microbiology 77, 8635-8647.

Karner, M.B., DeLong, E.F., Karl, D.M., 2001. Archaeal dominance in the mesopelagic zone of the Pacific Ocean. Nature 409, 507-510.

Keough, B., Schmidt, T., Hicks, R., 2003. Archaeal nucleic acids in picoplankton from great lakes on three continents. Microbial Ecology 46, 238-248.

Kim, J.-G., Jung, M.-Y., Park, S.-J., Rijpstra, W.I.C., Sinninghe Damsté, J.S., Madsen, E.L., Min, D., Kim, J.-S., Kim, G.-J., Rhee, S.-K., 2012. Cultivation of a highly enriched ammonia-oxidizing archaeon of thaumarchaeotal group I.1b from an agricultural soil. Environmental Microbiology 14, 1528-1543.

Kim, J.-H., Van der Meer, J., Schouten, S., Helmke, P., Willmott, V., Sangiorgi, F., Koç, N., Hopmans, E.C., Damsté, J.S.S., 2010. New indices and calibrations derived from the distribution of crenarchaeal isoprenoid tetraether lipids: Implications for past sea surface temperature reconstructions. Geochimica et Cosmochimica Acta 74, 4639-4654.

Lehtovirta-Morley, L.E., Stoecker, K., Vilcinskas, A., Prosser, J.I., Nicol, G.W., 2011. Cultivation of an obligate acidophilic ammonia oxidizer from a nitrifying acid soil. Proceedings of the National Academy of Sciences 108, 15892-15897.

Lincoln, S.A., Wai, B., Eppley, J.M., Church, M.J., Summons, R.E., DeLong, E.F., 2014a. Planktonic Euryarchaeota are a significant source of archaeal tetraether lipids in the ocean. Proceedings of the National Academy of Sciences 111, 9858-9863.

Lincoln, S.A., Wai, B., Eppley, J.M., Church, M.J., Summons, R.E., DeLong, E.F., 2014b. Reply to Schouten et al.: Marine Group II planktonic Euryarchaeota are significant contributors to tetraether lipids in the ocean. Proceedings of the National Academy of Sciences of the United States of America 111, E4286.

Liu, W., Wang, H., Zhang, C.L., Liu, Z., He, Y., 2013. Distribution of glycerol dialkyl glycerol tetraether lipids along an altitudinal transect on Mt. Xiangpi, NE Qinghai-Tibetan Plateau, China. Organic Geochemistry 57, 76-83.

Liu, X., Dong, H., Rech, J.A., Ryo, M., Yang, B., Wang, Y., 2008. Evolution of Chaka Salt Lake in NW China in response to climatic change during the Latest Pleistocene–Holocene. Quaternary Science Reviews 27, 867-879.

Loomis, S.E., Russell, J.M., Damsté, J.S.S., 2011. Distributions of branched GDGTs in soils and lake sediments from western Uganda: implications for a lacustrine paleothermometer. Organic Geochemistry 42, 739-751.

Loomis, S.E., Russell, J.M., Ladd, B., Street-Perrott, F.A., Sinninghe Damsté, J.S., 2012. Calibration and application of the branched GDGT temperature proxy on East African lake sediments. Earth and Planetary Science Letters 357–358, 277-288.

Loomis, S.E., Russell, J.M., Heureux, A.M., D'Andrea, W.J., Sinninghe Damsté, J.S., 2014. Seasonal variability of branched glycerol dialkyl glycerol tetraethers (brGDGTs) in a temperate lake system. Geochimica et Cosmochimica Acta 144, 173-187.

Naeher, S., Smittenberg, R.H., Gilli, A., Kirilova, E.P., Lotter, A.F., Schubert, C.J., 2012. Impact of recent lake eutrophication on microbial community changes as revealed by high resolution lipid biomarkers in Rotsee (Switzerland). Organic Geochemistry 49, 86-95.

Naeher, S., Peterse, F., Smittenberg, R.H., Niemann, H., Zigah, P.K., Schubert, C.J., 2014. Sources of glycerol dialkyl glycerol tetraethers (GDGTs) in catchment soils, water column and sediments of Lake Rotsee (Switzerland) – Implications for the application of GDGT-based proxies for lakes. Organic Geochemistry 66, 164-173.

Niemann, H., Stadnitskaia, A., Wirth, S., Gilli, A., Anselmetti, F., Sinninghe Damsté, J., Schouten, S., Hopmans, E., Lehmann, M., 2012. Bacterial GDGTs in Holocene sediments and catchment soils of a high Alpine lake: application of the MBT/CBT-paleothermometer. Climate of the Past 8, 889-906.

Pancost, R., Hopmans, E., Sinninghe Damste, J., Woodside, J., 2001. Archaeal lipids in Mediterranean cold seeps: molecular proxies for anaerobic methane oxidation.

Pearson, A., Ingalls, A.E., 2013. Assessing the use of archaeal lipids as marine environmental proxies. Annual Review of Earth and Planetary Sciences 41, 359-384.

Pearson, E.J., Juggins, S., Talbot, H.M., Weckström, J., Rosén, P., Ryves, D.B., Roberts, S.J., Schmidt, R., 2011. A lacustrine GDGT-temperature calibration from the Scandinavian Arctic to Antarctic: renewed potential for the application of GDGT-paleothermometry in lakes. Geochimica et Cosmochimica Acta 75, 6225-6238.

Peterse, F., Kim, J.-H., Schouten, S., Kristensen, D.K., Koç, N., Sinninghe Damsté, J.S., 2009. Constraints on the application of the MBT/CBT palaeothermometer at high latitude environments (Svalbard, Norway). Organic Geochemistry 40, 692-699.

Peterse, F., Nicol, G.W., Schouten, S., Sinninghe Damsté, J.S., 2010. Influence of soil pH on the abundance and distribution of core and intact polar lipid-derived branched GDGTs in soil. Organic Geochemistry 41, 1171-1175.

Peterse, F., van der Meer, J., Schouten, S., Weijers, J.W., Fierer, N., Jackson, R.B., Kim, J.-H., Damsté, J.S.S., 2012. Revised calibration of the MBT–CBT paleotemperature proxy based on branched tetraether membrane lipids in surface soils. Geochimica et Cosmochimica Acta 96, 215-229.

Peterse, F., Vonk, J.E., Holmes, R.M., Giosan, L., Zimov, N., Eglinton, T.I., 2014. Branched glycerol dialkyl glycerol tetraethers in Arctic lake sediments: Sources and implications for paleothermometry at high latitudes. Journal of Geophysical Research: Biogeosciences 119, 2014JG002639.

Pitcher, A., Rychlik, N., Hopmans, E.C., Spieck, E., Rijpstra, W.I.C., Ossebaar, J., Schouten, S., Wagner, M., Damsté, J.S.S., 2010. Crenarchaeol dominates the membrane lipids of Candidatus Nitrososphaera gargensis, a thermophilic Group I. 1b Archaeon. The ISME journal 4, 542-552.

Powers, L., Werne, J.P., Vanderwoude, A.J., Damsté, J.S.S., Hopmans, E.C., Schouten, S., 2010. Applicability and calibration of the TEX 86 paleothermometer in lakes. Organic Geochemistry 41, 404-413.

Schoon, P.L., de Kluijver, A., Middelburg, J.J., Downing, J.A., Sinninghe Damsté, J.S., Schouten, S., 2013. Influence of lake water pH and alkalinity on the distribution of core and intact polar branched glycerol dialkyl glycerol tetraethers (GDGTs) in lakes. Organic Geochemistry 60, 72-82.

Schouten, S., Hopmans, E.C., Schefuß, E., Sinninghe Damsté, J.S., 2002. Distributional variations in marine crenarchaeotal membrane lipids: a new tool for reconstructing ancient sea water temperatures? Earth and Planetary Science Letters 204, 265-274.

Schouten, S., Hopmans, E.C., Sinninghe Damsté, J.S., 2013. The organic geochemistry of glycerol dialkyl glycerol tetraether lipids: A review. Organic Geochemistry 54, 19-61.

Schouten, S., Villanueva, L., Hopmans, E.C., van der Meer, M.T., Damsté, J.S.S., 2014. Are Marine Group II Euryarchaeota significant contributors to tetraether lipids in the ocean? Proceedings of the National Academy of Sciences of the United States of

America 111, E4285.

Shanahan, T.M., Hughen, K.A., Van Mooy, B.A.S., 2013. Temperature sensitivity of branched and isoprenoid GDGTs in Arctic lakes. Organic Geochemistry 64, 119-128.

Sinninghe Damsté, J.S., Hopmans, E.C., Pancost, R.D., Schouten, S., Geenevasen, J.A., 2000. Newly discovered non-isoprenoid glycerol dialkyl glycerol tetraether lipids in sediments. Chemical Communications, 1683-1684.

Sinninghe Damsté, J.S., Rijpstra, W.I.C., Hopmans, E.C., Prahl, F.G., Wakeham, S.G., Schouten, S., 2002. Distribution of Membrane Lipids of Planktonic Crenarchaeota in the Arabian Sea. Applied and Environmental Microbiology 68, 2997-3002.

Sinninghe Damsté, J.S., Ossebaar, J., Abbas, B., Schouten, S., Verschuren, D., 2009. Fluxes and distribution of tetraether lipids in an equatorial African lake: constraints on the application of the TEX 86 palaeothermometer and BIT index in lacustrine settings. Geochimica et Cosmochimica Acta 73, 4232-4249.

Sinninghe Damsté, J.S., Rijpstra, W.I.C., Hopmans, E.C., Weijers, J.W.H., Foesel, B.U., Overmann, J., Dedysh, S.N., 2011. 13,16-Dimethyl Octacosanedioic Acid (iso-Diabolic Acid), a Common Membrane-Spanning Lipid of Acidobacteria Subdivisions 1 and 3. Applied and Environmental Microbiology 77, 4147-4154.

Sinninghe Damsté, J.S., Ossebaar, J., Schouten, S., Verschuren, D., 2012a. Distribution of tetraether lipids in the 25-ka sedimentary record of Lake Challa: extracting reliable TEX86 and MBT/CBT palaeotemperatures from an equatorial African lake. Quaternary Science Reviews 50, 43-54.

Sinninghe Damsté, J.S., Rijpstra, W.I.C., Hopmans, E.C., Jung, M.-Y., Kim, J.-G., Rhee, S.-K., Stieglmeier, M., Schleper, C., 2012b. Intact Polar and Core Glycerol Dibiphytanyl Glycerol Tetraether Lipids of Group I.1a and I.1b Thaumarchaeota in Soil. Applied and Environmental Microbiology 78, 6866-6874.

Sinninghe Damsté, J.S., Rijpstra, W.I.C., Hopmans, E.C., Foesel, B.U., Wüst, P.K., Overmann, J., Tank, M., Bryant, D.A., Dunfield, P.F., Houghton, K., Stott, M.B., 2014. Ether- and Ester-Bound iso-Diabolic Acid and Other Lipids in Members of Acidobacteria Subdivision 4. Applied and Environmental Microbiology 80, 5207-5218.

Sun, Q., Chu, G., Liu, M., Xie, M., Li, S., Ling, Y., Wang, X., Shi, L., Jia, G., Lü, H., 2011. Distributions and temperature dependence of branched glycerol dialkyl glycerol tetraethers in recent lacustrine sediments from China and Nepal. Journal of Geophysical Research: Biogeosciences (2005–2012) 116.

Tierney, J.E., Russell, J.M., Huang, Y., Damsté, J.S.S., Hopmans, E.C., Cohen, A.S., 2008. Northern hemisphere controls on tropical southeast African climate during the past 60,000 years. Science 322, 252-255.

Tierney, J.E., Russell, J.M., 2009. Distributions of branched GDGTs in a tropical lake system: Implications for lacustrine application of the MBT/CBT paleoproxy. Organic Geochemistry 40, 1032-1036.

Tierney, J.E., Mayes, M.T., Meyer, N., Johnson, C., Swarzenski, P.W., Cohen, A.S., Russell, J.M., 2010a. Late-twentieth-century warming in Lake Tanganyika unprecedented since AD 500. Nature Geoscience 3, 422-425.

Tierney, J.E., Russell, J.M., Eggermont, H., Hopmans, E., Verschuren, D., Damsté, J.S., 2010b. Environmental controls on branched tetraether lipid distributions in tropical East African lake sediments. Geochimica et Cosmochimica Acta 74, 4902-4918.

Turich, C., Freeman, K.H., 2011. Archaeal lipids record paleosalinity in hypersaline systems. Organic Geochemistry 42, 1147-1157.

Tyler, J.J., Nederbragt, A.J., Jones, V.J., Thurow, J.W., 2010. Assessing past temperature and soil pH estimates from bacterial tetraether membrane lipids: Evidence from the recent lake sediments of Lochnagar, Scotland. Journal of Geophysical Research: Biogeosciences 115, G01015.

Wang, H., Liu, W., Zhang, C.L., Wang, Z., Wang, J., Liu, Z., Dong, H., 2012. Distribution of glycerol dialkyl glycerol tetraethers in surface sediments of Lake Qinghai and surrounding soil. Organic Geochemistry 47, 78-87.

Wang, H., Liu, W., Zhang, C.L., Jiang, H., Dong, H., Lu, H., Wang, J., 2013. Assessing the ratio of archaeol to caldarchaeol as a salinity proxy in highland lakes on the northeastern Qinghai–Tibetan Plateau. Organic Geochemistry 54, 69-77.

Weijers, J.W.H., Schouten, S., Hopmans, E.C., Geenevasen, J.A.J., David, O.R.P., Coleman, J.M., Pancost, R.D., Sinninghe Damsté, J.S., 2006. Membrane lipids of mesophilic anaerobic bacteria thriving in peats have typical archaeal traits. Environmental Microbiology 8, 648-657.

Weijers, J.W.H., Schouten, S., van den Donker, J.C., Hopmans, E.C., Sinninghe Damsté, J.S., 2007. Environmental controls on bacterial tetraether membrane lipid distribution in soils. Geochimica et Cosmochimica Acta 71, 703-713.

Woltering, M., Johnson, T.C., Werne, J.P., Schouten, S., Damsté, J.S.S., 2011. Late Pleistocene temperature history of Southeast Africa: a TEX 86 temperature record from Lake Malawi. Palaeogeography, Palaeoclimatology, Palaeoecology 303, 93-102.

Xie, S., Pancost, R.D., Chen, L., Evershed, R.P., Yang, H., Zhang, K., Huang, J., Xu, Y., 2012. Microbial lipid records of highly alkaline deposits and enhanced aridity associated with significant uplift of the Tibetan Plateau in the Late Miocene. Geology 40, 291-294.

Yang, H., Ding, W., Wang, J., Jin, C., He, G., Qin, Y., Xie, S., 2012. Soil pH impact on microbial tetraether lipids and terrestrial input index (BIT) in China. Science China Earth Sciences 55, 236-245.

Yang, H., Pancost, R.D., Dang, X., Zhou, X., Evershed, R.P., Xiao, G., Tang, C., Gao, L., Guo, Z., Xie, S., 2014. Correlations between microbial tetraether lipids and environmental variables in Chinese soils: Optimizing the paleo-reconstructions in semi-arid and arid regions. Geochimica et Cosmochimica Acta 126, 49-69.

Yang, H., Pancost, R.D., Jia, C., Xie, S., 2016. The Response of Archaeal Tetraether Membrane Lipids in Surface Soils to Temperature: A Potential Paleothermometer in Paleosols. Geomicrobiology Journal 33, 98-109.

Yang, J., Jiang, H., Dong, H., Wang, H., Wu, G., Hou, W., Liu, W., Zhang, C., Sun, Y., Lai, Z., 2013. amoA-encoding archaea and thaumarchaeol in the lakes on the northeastern Qinghai-Tibetan Plateau, China. Frontiers in microbiology 4.

Zell, C., Kim, J.-H., Moreira-Turcq, P., Abril, G., Hopmans, E.C., Bonnet, M.-P., Sobrinho, R.L., Damsté, J.S.S., 2013. Disentangling the origins of branched tetraether lipids and crenarchaeol in the lower Amazon River: Implications for GDGT‐based proxies. Limnology and Oceanography 58, 343-353.

Zheng, X., Zhang, M., Li, B., Xu, C., 2002. Salt lakes of China. Beijing: Science Press.

Tables

Table 1

Fractional abundance of isoGDGTs and isoGDGT-based proxies for river sediments (RS), lake sediments (LS) and soils (S) in and around Chaka Salt Lake

Sample	Lat.(N)	Long.(E)	Fractional abundance of isoGDGTs (%)						Total isoGDGTs (μg/g TOC)	TOC(%)	BIT	$R_{i/b}$	TEX_{86}	cren/cren'	GDGT-0/cren	ACE
			GDGT-0	GDGT-1	GDGT-2	GDGT-3	cren	cren'								
RS1	36°47.496′	99°01.296′	55.8	5.3	7.4	3.4	25.9	2.2	1.09	1.84	0.69	1.28	0.71	11.84	2.16	0.11
RS2	36°47.368′	99°01.293′	78.9	3.7	4.0	1.4	11.1	0.9	2.04	1.34	0.91	0.63	0.63	13.00	7.10	0.01
RS3	36°47.219′	99°01.304′	66.4	5.0	6.3	2.7	18.1	1.5	0.58	1.58	0.80	0.89	0.68	12.21	3.66	0.07
RS4	36°46.801′	99°01.329′	49.5	6.9	9.2	3.6	29.0	1.8	1.11	0.83	0.69	0.98	0.68	16.21	1.71	0.18
LS5	36°44.719′	99°03.379′	71.6	19.5	6.1	1.2	1.4	0.1	2.56	1.71	0.81	14.35	0.28	11.13	52.41	0.16
LS6	36°44.913′	99°02.839′	54.9	5.8	8.2	3.9	25.2	1.9	1.60	0.97	0.76	0.92	0.71	13.06	2.18	0.43
LS7	36°44.768′	99°02.896′	45.2	6.4	9.7	4.3	31.8	2.6	0.52	2.03	0.56	1.81	0.72	12.24	1.42	0.66
LS8	36°44.366′	99°02.752′	74.2	17.2	5.2	1.2	2.0	0.2	0.99	1.60	0.81	10.02	0.28	10.91	38.00	0.16
LS9	36°44.309′	99°02.765′	69.6	16.9	6.7	2.0	4.3	0.5	0.51	1.39	0.79	4.99	0.35	8.51	16.33	0.43
LS10	36°44.526′	99°02.704′	28.2	12.2	12.5	8.5	32.6	6.0	0.06	2.67	0.36	2.43	0.69	5.47	0.86	0.63
S11	36°43.509′	98°52.185′	25.6	7.8	12.6	4.4	47.6	2.0	1.05	0.79	0.52	1.79	0.71	23.51	0.54	0.01
S12	36°43.525′	98°52.157′	21.4	8.0	15.6	5.8	45.0	4.2	0.82	0.81	0.70	0.90	0.76	10.74	0.48	0.14
S13	36°43.352′	98°52.245′	52.7	5.4	6.4	2.4	31.8	1.4	0.68	0.86	0.53	2.65	0.65	23.03	1.66	0.01
S14	36°40.906′	98°52.673′	33.7	7.8	9.4	3.4	44.3	1.5	0.51	2.26	0.49	2.28	0.65	29.86	0.76	0.00
S15	36°41.176′	98°53.049′	79.8	2.7	3.4	1.4	12.1	0.6	0.08	1.30	0.62	4.80	0.66	21.66	6.60	0.01

Table 2

Fractional abundance of brGDGTs and brGDGT-based proxies for river sediments (RS), lake sediments (LS) and soils (S) in and around Chaka Salt Lake

Sample	Lat.(N)	Long.(E)	Fractional abundance of brGDGTs (%)									Total brGDGTs (μg/g TOC)	TOC(%)	MBT	CBT	MBT'
			III	IIIb	IIIc	II	IIb	IIc	I	Ib	Ic					
RS1	36°47.496′	99°01.296′	33.6	1.9	0.2	29.3	13.4	1.6	9.6	5.4	5.0	0.85	1.84	0.20	0.31	0.20
RS2	36°47.368′	99°01.293′	30.3	1.9	0.3	35.0	15.2	0.9	7.7	7.9	0.9	3.27	1.34	0.17	0.27	0.17
RS3	36°47.219′	99°01.304′	28.8	3.0	0.5	27.6	16.0	2.4	8.6	9.1	4.0	0.64	1.58	0.22	0.16	0.23
RS4	36°46.801′	99°01.329′	27.5	3.4	0.6	26.8	18.9	2.7	8.4	8.0	3.8	1.13	0.83	0.20	0.12	0.21
LS5	36°44.719′	99°03.379′	50.0	2.9	0.3	27.0	7.5	0.8	9.1	1.8	0.7	0.18	1.71	0.12	0.59	0.12
LS6	36°44.913′	99°02.839′	30.8	3.3	0.6	32.5	16.9	1.6	8.3	4.9	0.9	1.74	0.97	0.14	0.27	0.15
LS7	36°44.768′	99°02.896′	34.0	2.9	0.4	31.9	15.4	1.3	7.7	5.1	1.3	0.29	2.03	0.14	0.29	0.15
LS8	36°44.366′	99°02.752′	48.5	3.5	0.9	24.8	7.3	1.1	8.9	3.3	1.8	0.10	1.60	0.14	0.50	0.15
LS9	36°44.309′	99°02.765′	45.4	2.4	0.0	25.7	10.6	2.5	6.7	3.9	2.7	0.10	1.39	0.13	0.35	0.14
LS10	36°44.526′	99°02.704′	12.6	2.5	0.0	25.2	25.5	6.8	6.3	11.4	9.7	0.03	2.67	0.27	-0.07	0.28
S11	36°43.509′	98°52.185′	50.6	1.2	0.1	37.6	1.5	1.8	5.0	0.5	1.6	0.59	0.79	0.07	1.33	0.07
S12	36°43.525′	98°52.157′	53.0	1.4	0.2	36.5	2.4	0.5	4.8	0.5	0.5	0.91	0.81	0.06	1.14	0.06
S13	36°43.352′	98°52.245′	45.0	0.8	0.3	45.4	1.6	0.7	5.6	0.6	0.0	0.26	0.86	0.06	1.38	0.06
S14	36°40.906′	98°52.673′	53.8	0.5	0.0	37.0	1.1	1.7	4.5	0.3	1.2	0.22	2.26	0.06	1.47	0.06
S15	36°41.176′	98°53.049′	45.9	0.0	0.0	39.8	4.9	1.8	7.5	0.0	0.0	0.02	1.30	0.08	0.98	0.08

Figure Captions

Fig.1. Chemical structures and molecular ion *m/z* values for glycerol dialkyl glycerol tetraethers (GDGTs) and archaeol.

Fig.2. Map of Chaka Salt Lake showing locations of samples. Sampling sites correspond to Table 1 and Table 2.

Fig.3. Fractional abundance of GDGT 0-3, crenarchaeol, crenarchaeol' and GDGT I-III as fractions of the sum of all GDGTs in river sediments, lake sediments and soils.

Fig.4. Box plot showing scale values of cren/cren' in soil, lake sediments and marine sediments, as well as Thaumarchaeota Group I.1a and Group I.1b from published literature (De La Torre et al., 2008, Blaga et al., 2009, Kim et al., 2010, Jung et al., 2011, Lehtovirta-Morley et al., 2011, Kim et al., 2012, Sinninghe Damsté et al., 2012b, Wang et al., 2012, Yang et al., 2012).

Fig.5. Plots showing the distributions of MBT and CBT indices in river sediments, lake sediments and soils.

Fig.6. Comparison of reconstructed temperature based on lake TEX_{86} calibrations in lake sediments as listed from Eq. 8 to Eq. 12.

Fig.7. Comparison of reconstructed temperature based on soil calibrations in soils, river sediments and lake sediments as listed from Eq. 13 to Eq. 16.

Fig.8. Comparison of reconstructed temperature based on lake calibrations as listed

from Eq. 17 to Eq. 23. Calibrations of MBT/CBT and fractional abundance of branched GDGTs were applied to river sediments and lake sediments.

Figure 1

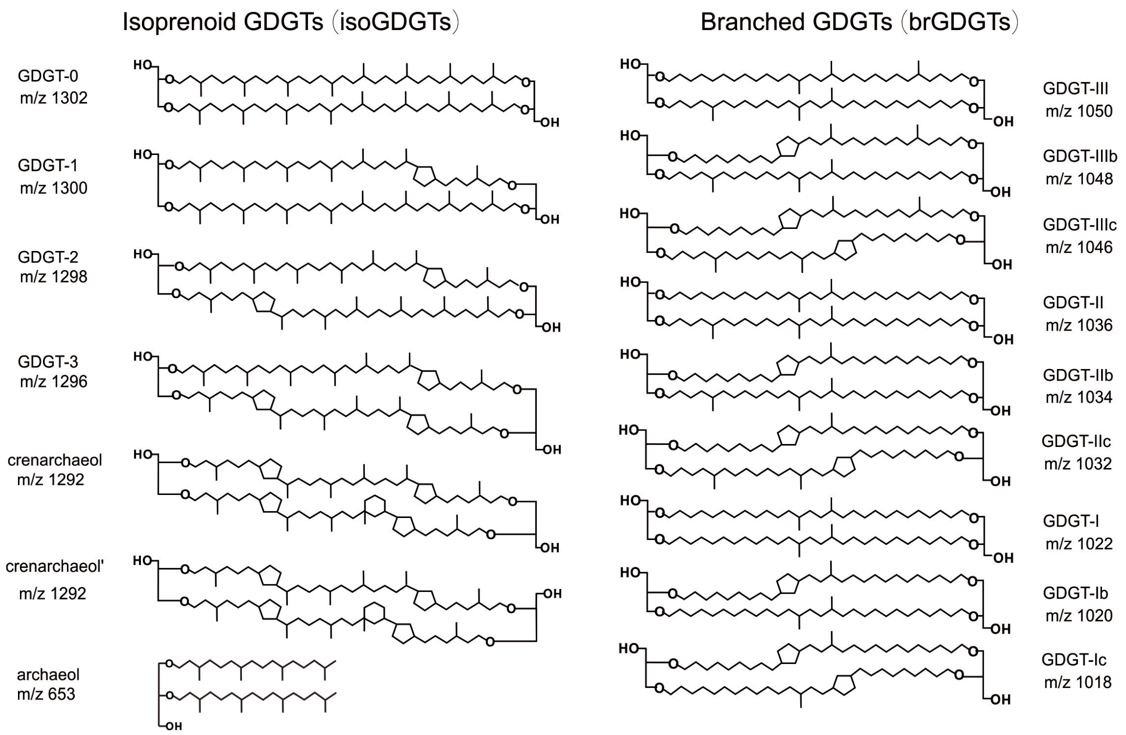
Isoprenoid GDGTs (isoGDGTs)
Branched GDGTs (brGDGTs)
GDGT-0
m/z 1302
GDGT-1
m/z 1300
GDGT-2
m/z 1298
GDGT-3
m/z 1296
crenarchaeol
m/z 1292
crenarchaeol'
m/z 1292
archaeol
m/z 653
GDGT-III
m/z 1050
GDGT-IIIb
m/z 1048
GDGT-IIIc
m/z 1046
GDGT-II
m/z 1036
GDGT-IIb
m/z 1034
GDGT-IIc
m/z 1032
GDGT-I
m/z 1022
GDGT-Ib
m/z 1020
GDGT-Ic
m/z 1018

870 Figure 2

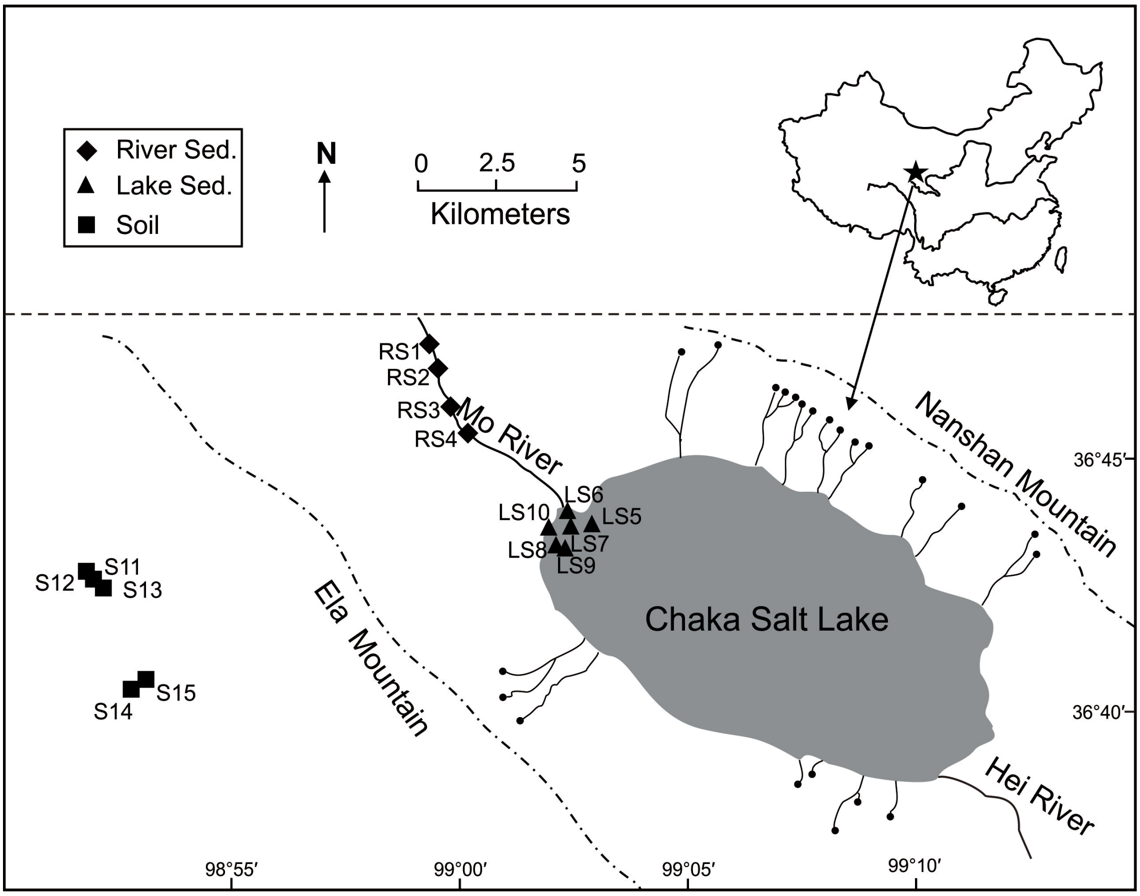

871

Figure 3

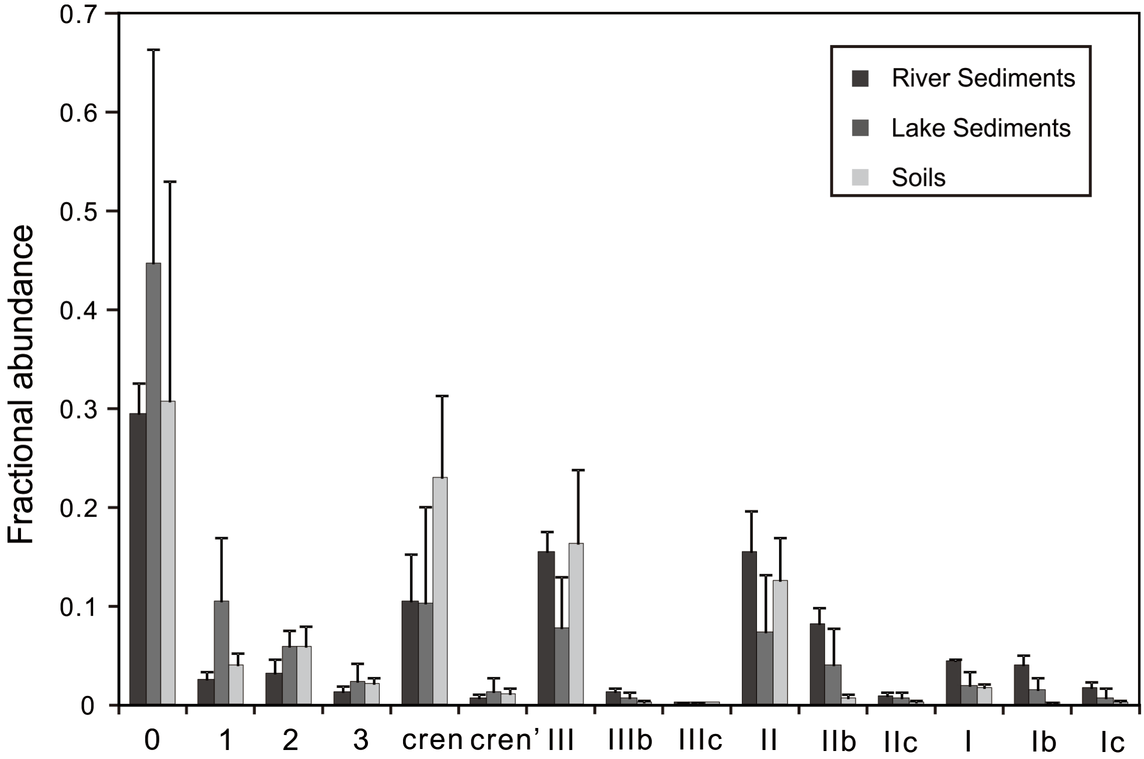
River Sediments
Lake Sediments
Soils
Fractional abundance
0.7
0.6
0.5
0.4
0.3
0.2
0.1
0
0
1
2
3
cren
cren'
III
IIIb
IIIc
II
IIb
IIc
I
Ib
Ic

Figure 4

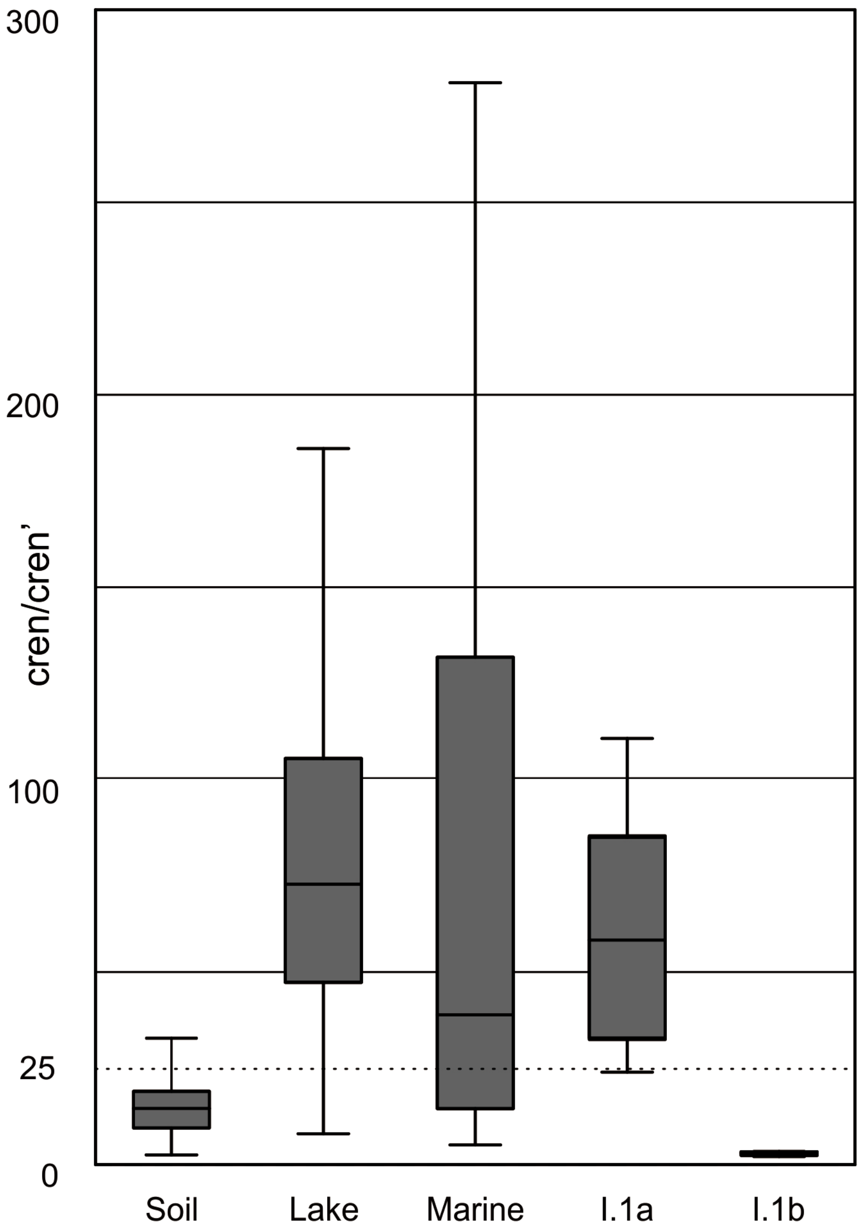

Figure 5

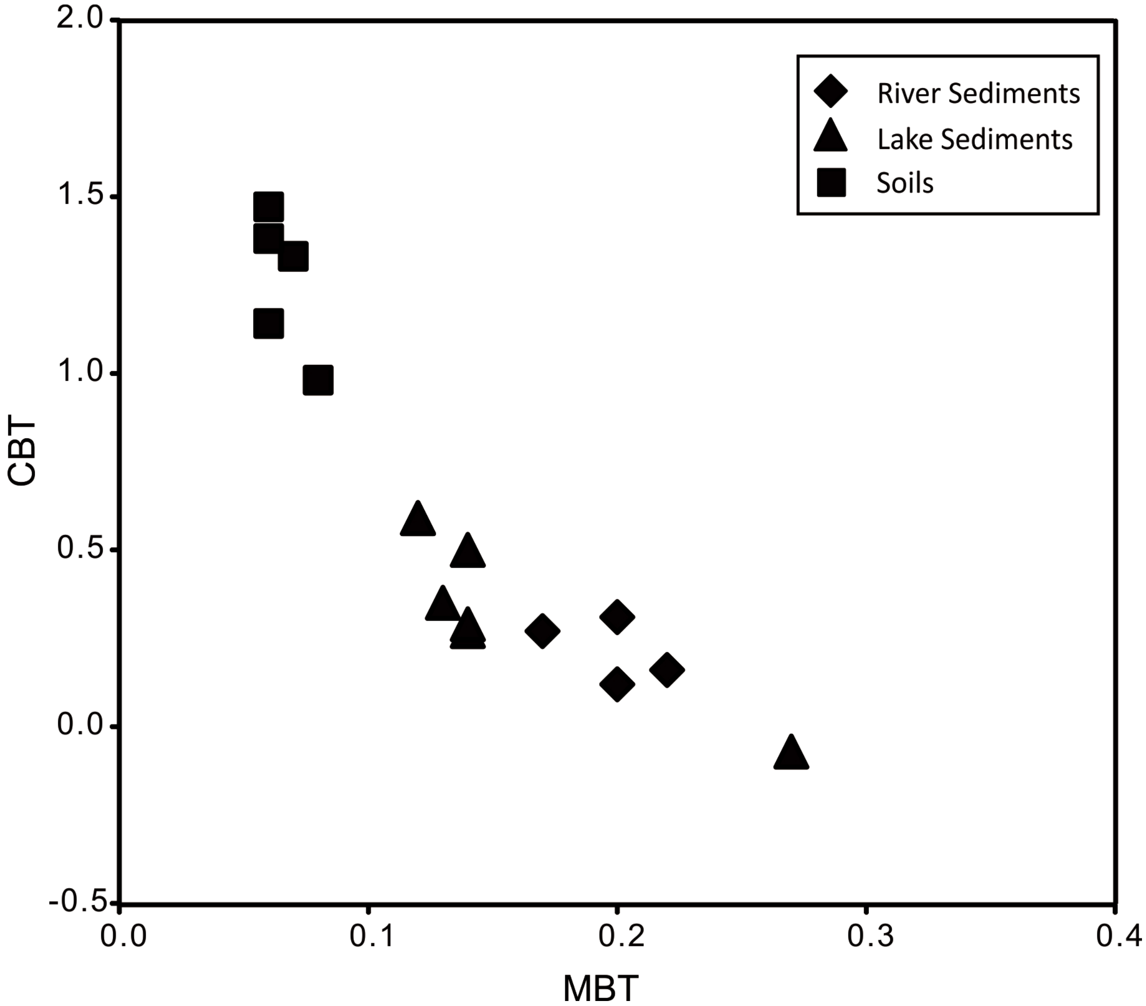
River Sediments
Lake Sediments
Soils
CBT
2.0
1.5
1.0
0.5
0.0
-0.5
0.0
0.1
0.2
0.3
0.4
MBT

Figure 6

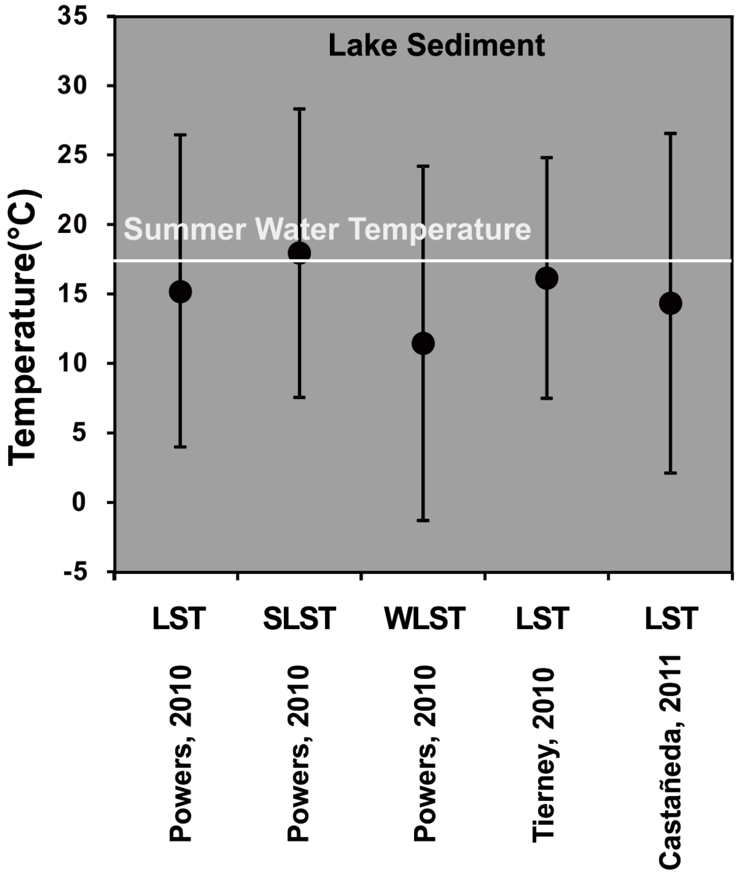
Lake Sediment
Summer Water Temperature
Temperature(°C)
35
30
25
20
15
10
5
0
-5
LST
SLST
WLST
LST
LST
Powers, 2010
Powers, 2010
Powers, 2010
Tierney, 2010
Castañeda, 2011

Figure 7

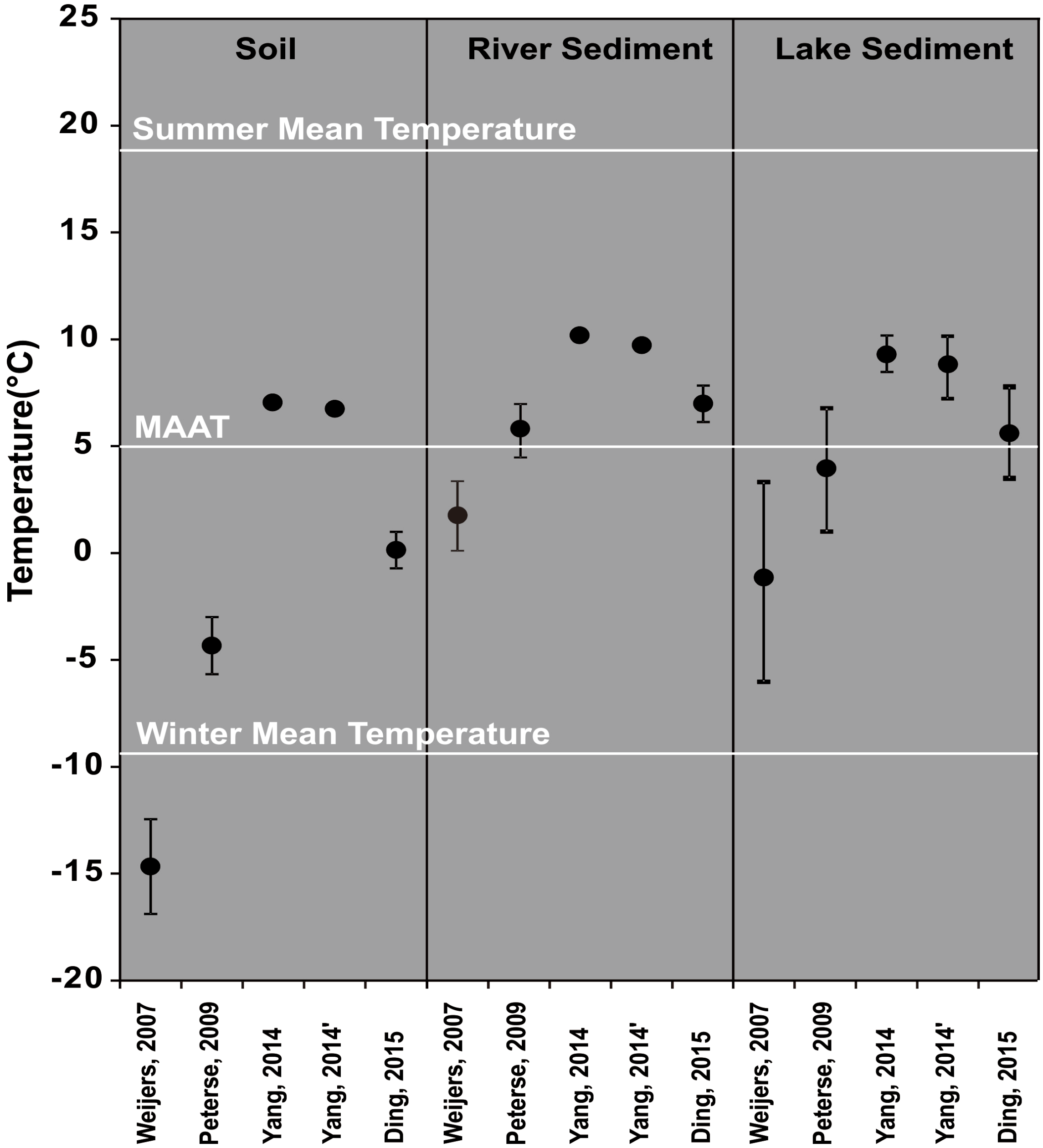
Soil
River Sediment
Lake Sediment
Summer Mean Temperature
MAAT
Winter Mean Temperature
Temperature(°C)
25
20
15
10
5
0
-5
-10
-15
-20
Weijers, 2007
Peterse, 2009
Yang, 2014
Yang, 2014'
Ding, 2015
Weijers, 2007
Peterse, 2009
Yang, 2014
Yang, 2014'
Ding, 2015
Weijers, 2007
Peterse, 2009
Yang, 2014
Yang, 2014'
Ding, 2015

888 Figure 8

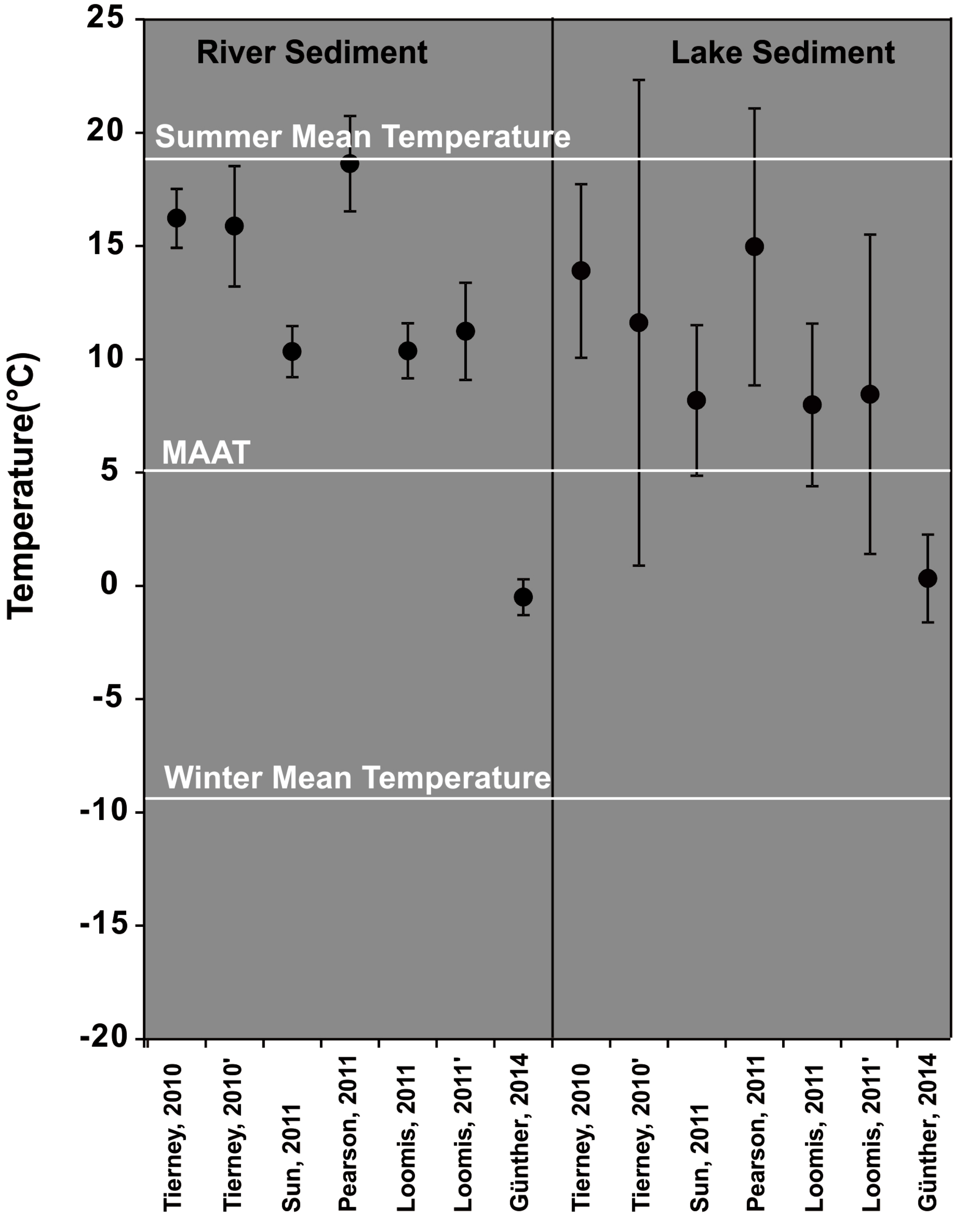

889